Published in final edited form as:
J Nucl Cardiol. 2011 May ; 18(3): 443–450. doi:10.1007/s12350-011-9369-9.

Myocardial substrate and route of administration determine acute cardiac retention and lung bio-distribution of cardiosphere-derived cells

Michael Bonios, MD[a], **John Terrovitis, MD**[a], **Connie Y. Chang, MSE**[a], **James M. Engles, MS, MBA**[a], **Takahiro Higuchi, MD, PhD**[a], **Riikka Lautamäki, MD**[a], **Jianhua Yu, BS**[a], **James Fox, BS**[a], **Martin Pomper, MD, PhD**[a], **Richard L. Wahl, MD**[a], **Benjamin M. Tsui, PhD**[a], **Brian O'Rourke, MD, PhD**[a], **Frank M. Bengel, MD**[a], **Eduardo Marbán, MD, PhD**[b], and **M. Roselle Abraham, MD**[a]

[a]Johns Hopkins University Baltimore, MD

[b]Cedars-Sinai Heart Institute, Los Angeles, CA

Abstract

Background—Quantification of acute myocardial retention and lung bio-distribution of cardiosphere-derived cells (CDCs) following transplantation is important to improve engraftment.

Methods and results—We studied acute(1 hour) cardiac/lung retention in 4 groups (n = 25) of rats (normal—*NL*, acute ischemia-reperfusion—*AI-RM*, acute permanent ligation—*PL*, and chronic infarct by ischemia-reperfusion—*CI-R*) using intra-myocardial delivery, 1 group using intracoronary delivery (acute ischemia-reperfusion, *AI-RC*, n = 5) and 1 group using intravenous delivery (acute ischemia-reperfusion, *AI-RV*, n = 5) of CDCs by PET. Cardiac retention was similar in the NL, AI-RM, CI-R, and A-IRC groups (13.6% ± 2.3% vs 12.0% ± 3.9% vs 9.9 ± 2.8 vs 15.4% ± 5.5%; *P* = NS), but higher in PL animals (22.9% ± 5.2%; *P* < .05). Low cardiac retention was associated with significantly higher lung activity in NL and AI-RM groups (43.3% ± 5.6% and 39.9% ± 9.3%), compared to PL (28.5% ± 5.9%), CI-R (20.2% ± 9.3%), and A-IRC (19.9% ± 5.6%) animals (*P* < .05 vs AI-RM and NL). Lung activity was highest following intravenous CDC delivery (55.1% ± 9.3%, *P* < .001) and was associated with very low cardiac retention (0.8% ± 1.06%). Two-photon microscopy indicated that CDCs escaped to the lungs via the coronary veins following intra-myocardial injection.

Conclusions—Acute cardiac retention and lung bio-distribution vary with the myocardial substrate and injection route. Intra-myocardially injected CDCs escape into the lungs via coronary veins, an effect that is more pronounced in perfused myocardium.

Reprint requests: M. Roselle Abraham, MD, Johns Hopkins University, 720 Rutland Ave, Ross 871, Baltimore, MD 21210; mabraha3@jhmi.edu.

Michael Bonios and John Terrovitis equally contributed to this work.

Electronic supplementary material The online version of this article (doi:10.1007/s12350-011-9369-9) contains supplementary material, which is available to authorized users.

Disclosures

Dr. Eduardo Marbán is founder and equity holder of Capricor, Inc. that works on CDCs. Capricor provided no funding for the present study. The remaining authors report no conflicts.

Keywords

Stem cells; acute heart retention; PET; lung bio-distribution

INTRODUCTION

Stem cell transplantation holds promise for cardiac regeneration, both after acute myocardial infarction (MI) and in chronic cardiomyopathies. Despite the excitement surrounding cell therapy, clinical, and experimental studies of stem cell transplantation reveal low engraftment rates and marginal functional benefit in the long term.[1] Direct intra-myocardial injection into the left ventricular wall during cardiac surgery was the first route used for stem cell transplantation in both clinical and experimental studies.[2,3] It has the advantage of permitting delivery of large numbers of cells locally into the myocardium, and is believed to minimize escape of transplanted cells into the systemic circulation.[4] However, low engraftment was a common finding in experimental and clinical studies[5] even after direct intra-myocardial[6] administration, suggesting that quantification of myocardial retention of transplanted cells is necessary to help design strategies to improve engraftment and cardiac function in the long term.

In this study, we investigated cardiosphere-derived cells (CDCs), which are in phase 1 clinical trials (CADUCEUS). CDCs are progenitor cells derived from monolayer outgrowth of heart tissue and are comprised a mixture of c-kit^{+}/CD90^{-} cardiac progenitor cells and cardiac mesenchymal stem cells (c-kit^{-}/CD105^{+}, 90^{+}) that together have a synergistic effect on cardiac regeneration.[7] Previous studies by our group reveal low levels of acute retention (1-hour post-transplantation) and chronic engraftment.[8] However, the mechanisms underlying low acute myocardial cell retention have not been fully elucidated.

We performed in vivo positron emission tomography/computed tomography (PET/CT) to assess the determinants of acute myocardial retention and lung bio-distribution of CDCs. We chose PET because it combines the advantage of high sensitivity with the potential for accurate quantification[8] and can be translated into large animal models and patients.[9] We found that acute cardiac retention varies with the injection route and myocardial substrate; cardiac cell retention is highest following intra-myocardial injection in the infarcted heart after permanent ligation of the LAD, in comparison to normal and reperfused, infarcted myocardium. Large numbers of intra-myocardially injected CDCs escaped into the lungs acutely via the coronary venous system, an effect that was more pronounced in normal myocardium and following ischemia-reperfusion.

METHODS

Isolation of rCDCs, Tissue Culture and Cell Labeling

rCDCs were isolated from hearts of male, 3 month old, Wistar Kyoto (WKY) rats (Harlan, Indianapolis, Indiana, USA), as previously described,[7,10] and injected into female WKY rats. WKY rats are genetically identical, which makes them ideally suited for cell transplantation studies.[11] The use of gender-mismatched transplantation permits validation

of in vivo molecular imaging results by (quantitative) real-time PCR for the male-specific rat SRY gene.

In Vitro FDG Labeling

Tritiated ^{3}H[FDG], a beta emitter was used to measure FDG uptake in vitro; radiotoxicity of ^{18}FDG was assessed using the WST-8 assay (Supplemental material).

rCDC Injection Preparation

One million (intracoronary injections), two million (intra-myocardial injections), or five million (intravenous injections) rCDCs were labelled with ^{18}FDG immediately before injection, by the addition of 2 μCi ^{18}FDG/mL of glucose-free DMEM to adherent rCDCs for 30 minutes. Subsequently, labelling media was removed by two washes in PBS, rCDCs were trypsinized, pelleted by centrifugation, and suspended in PBS (Ca^{2+}- and Mg^{2+}-free) and transferred to the injection syringe (the maximum cell number and injectate volume that did not increase post-operative mortality were used).

Animal Surgery—Cell Injection

Female WK rats weighing 180–200 g were used as cell recipients. Rats were intubated, anesthesia was induced with 4% isoflurane inhalation and maintained with 2% inhalation. The heart was exposed through a left lateral thoracotomy, and animals were randomly assigned to several groups (Table 1). For ischemia reperfusion, the LAD was reversibly occluded for 45 minutes using a 5.0 mm silk suture and snare. Following cell injection, the chest was closed and animals were transferred to the PET scanner or allowed to recover in their cages for qPCR experiments.

Intra-myocardial rCDC delivery—We studied four groups of animals: permanent ligation of the LAD (PL: n = 7 for PET and n = 8 for qPCR), acute ischemia-reperfusion (AI-RM: n = 9 for PET and n = 8 for qPCR), chronic ischemia reperfusion (CI-R: CI-R, n = 5 for PET and n = 8 for qPCR), or normal (NL, n = 4 for PET and n = 6 for qPCR) group; 2 × 10^{6} rCDCs, suspended in 100 μL of PBS, were injected intra-myocardially into two sites of the infarct region in the PL, AI-RM, and CI-R groups or into the anterior wall in the NL group, using a 28G needle.

Intracoronary rCDC delivery—In order to simulate intracoronary cell delivery, 1 × 10^{6} rCDCs suspended in 200 μL PBS were injected into the left ventricular cavity after transient cross clamp of the aorta[12] immediately after ischemia-reperfusion of the LAD (AI-RC, n = 5 for PET).

Intravenous rCDC delivery—Following ischemia-reperfusion of the LAD, the chest was closed and 5 × 10^{6} rCDCs suspended in 500 μL PBS were injected into the tail vein over 10 minutes (AI-RV, n = 5 for PET, n = 5 for qPCR).

All animals used in this study received humane care, in compliance with the “Guide for the Care and the Use of Laboratory Animals” published by the US National Institutes of Health.

PET/CT Imaging

PET images were acquired on a GE Healthcare Vista small animal PET system. In every experiment, the syringe containing ^{18}FDG-labelled rCDCs were imaged in the PET scanner using a 5-minute static acquisition before and after cell injection to measure residual activity and calculate the net injected activity, corresponding to the cell number injected in each animal. Animals were anaesthetized and placed head first in the PET scanner. ^{18}FDG images were obtained as dynamic, list mode acquisitions. For myocardial delineation and accurate quantification of activity exclusively derived from rCDCs retained in the myocardium, a perfusion PET scan (20-minute static acquisition) was performed following injection of 37 MBq of $^{13}NH_3$ at the end of the FDG acquisition. Free ^{18}F (37 mBq) was injected after completion of the $^{13}NH_3$ acquisition to facilitate co-registration of PET images with CT and allow quantification of the signal (see Supplemental material for imaging and image analysis details).

Real-Time Quantitative Polymerase Chain Reaction (qPCR)

Quantitative PCR—The results obtained by in vivo PET following intra-myocardial injection and intravenous rCDC injection were validated using quantitative PCR for the male-specific SRY gene in a separate set of experiments. For this purpose, animals were killed 1 hour following rCDC transplantation, the heart and lungs were explanted, weighed, and homogenized (Supplemental material).

Fluorescence Microscopy

We performed ex vivo 2-photon microscopy of the rat heart to image the coronary microvasculature,[13–15] (Supplemental material).

Statistics

Values are reported as mean ± SD. The paired *t* test was used for comparisons of in vitro FDG uptake rates under different culture conditions. One-way ANOVA was used to compare %ID among the four groups (PL, AI-RM, NL, and CI-R) and the Tukey's multiple comparison post hoc test was used for inter-group comparisons. A $P < .05$ was chosen for statistical significance.

RESULTS

Radio-Labeling of rCDCs with ^{18}FDG

The doses, 0.2 μCi/mL and 2 μCi/mL of ^{18}FDG, had no effect on CDC viability and proliferation for up to 7 days after labeling (Figure 1A); however, all higher doses demonstrated significant toxicity, likely radiation-related. Based on these results, a dose of 2 μCi/mL of ^{18}FDG for 30 minutes was selected for further in vitro and in vivo experiments.

Cellular uptake of ^{3}H[FDG] was higher in adherent CDCs than CDCs in suspension (Figure 1B). In adherent CDCs, cellular uptake of ^{3}H[FDG] was 2.2% ± 1.3% of the administered dose at 30 minutes and reached a plateau thereafter (Figure 1C). Addition of insulin did not increase ^{3}H[FDG] uptake at 30 and 60 minutes (n = 2) (Figure 1C) in adherent cells, suggesting lack of GLUT4 expression in CDCs. RT-PCR confirmed that CDCs only express

GLUT1. Retention studies (n = 2) revealed that 79% ± 12% of the radioactivity persisted at 1 hour and 68% ± 0.02% at 4 hours after labeling, suggesting that only a small amount of ^{3}H[FDG] is not phosphorylated and leaks out of the cell (Figure 1D).

In Vivo PET Imaging

In all animals, the myocardium was successfully visualized by ^{13}NH3 (Figure 2A, green). The infarcted area appeared as a perfusion deficit in the anterolateral wall, while the injected cells appeared as bright spots within the perfusion deficit (Figure 2, yellow arrows).

Effect of an Open Infarct-Related Artery on CDC Retention Following Intra-Myocardial Injection

In vivo PET imaging—We found that acute cardiac retention following intra-myocardial injection varied with the infarct model: cell retention (% of net injected activity) in the heart at 1 hour was similar in the NL, AI-RM, and CI-R groups (13.6% ± 2.3% vs 12.0% ± 3.9% vs 9.9 ± 2.8; *P* = NS) but higher in the PL group (22.9% ± 5.2%) when compared to NL, AI-RM, and CI-R groups (*P* < .05) (Figure 2A–D; Supplemental Figures 1, 2). The main reason for low cardiac retention appears to be escaped from large numbers of injected CDCs into the lungs very early after injection. In fact, quantification of activity in the lungs was 39.9% ± 9.3% in the AI-RM group, 43.3% ± 5.6% in the NL group, 28.5% ± 5.0% in the PL group, and 20.2% ± 9.3% in the CI-R group (*P* < .05 for PL vs NL and AI-RM groups; *P* < .01 for CI-R vs NL and AI-RM groups), reflecting higher proportions of cells trapped in the lungs in the groups with lower cardiac retention (Figure 2E).

Real-time PCR—Real-time PCR performed 1 hour after CDC injection in a separate group of animals confirmed the results obtained by in vivo PET imaging. PCR also revealed higher numbers of CDCs in the lungs than the heart in the AI-RM and NL compared to PL and CI-R groups; the ratio of CDCs in the heart to lungs was 0.6 ± 0.1 in the AI-RM group, 0.9 ± 0.3 in the NL group, 0.7 ± 0.4 in the CI-R group, and 3.3 ± 3.2 in the PL group (*P* < .05 for PL vs AI-RM and C-IR groups).

Mechanism of CDC Loss After Intra-Myocardial Injection

We observed cell clumps transiting through the coronary sinus on several occasions during or immediately following intra-myocardial injection of CDCs, which prompted us to investigate the vasculature using 2-photon microscopy. Fluorescence microscopy revealed large numbers of Di-I labeled cells within the cardiac vasculature (labeled with thioflavin) distal from the injection site, in animals killed within 5 minutes of CDC injection, confirming that cell egress from the injection site occurs very early after cell delivery. Since thioflavin does not specifically label cardiac veins, we cannot rule out the possibility that cell egress also occurred via lymphatics into the cardiac venous system.

Effect of Delivery Route on CDC Bio-Distribution

Acute myocardial retention (Figure 3A, Supplemental Figure 3) with intracoronary delivery (by intra-cavitary CDC injection following cross-clamp of the aorta) following acute ischemia-reperfusion was quantitatively similar to that following intra-myocardial delivery

(15.4% ± 5.5%, $P > .05$ vs all other groups), but the distribution was spatially more widespread and heterogeneous (probably due to areas of microvascular obstruction induced by ischemia-reperfusion). However, lung activity was lower (19.9% ± 5.6%; $P < .01$ vs AI-RM and NL). In contrast, following intravenous delivery (Figure 3B), majority of injected cells (55.1% ± 9.33%) were trapped in the lungs, cardiac retention was very low (0.8% ± 1.06% by qPCR) and was not quantifiable by in vivo PET imaging.

DISCUSSION

The main findings of this study are[1] the myocardial substrate and route of transplantation influence acute CDC retention in the myocardium,[2] CDCs rapidly escape from intra-myocardial injection sites into the pulmonary circulation via the cardiac veins and are trapped in the lungs.

In this study, we used in vivo PET imaging, a method that is directly translatable to clinical studies, to quantify the signal derived from ^{18}FDG-labeled CDCs in the heart and lungs; PET results were validated using quantitative PCR. In this study and in accordance with previous reports,[3–5,16] cell retention at the injection site was relatively low following intra-myocardial injection (Figure 2A–D). Intra-myocardial injection can result in cell loss through the needle track, coronary venous vessels/coronary sinus, thebesian veins and through the endocardium into the left ventricular cavity.[17] We found that the most important mechanism of early cell loss is washout via the cardiac venous system, which was also reported by Anderl et al[17] using microspheres. We postulate that intramyocardial injection results in disruption of venules/veins at the site of needle insertion and consequent entry of the injectate/cells into the coronary venous system. Some of the cells that entered the coronary venous circulation eventually were trapped in the lung capillaries because of cell size, explaining why this organ was found to be the main extra-cardiac site of CDC localization when we performed whole body PET scans (Figure 2C). Similar findings have been reported in the past in studies where the fate of fluorescent or radioactive microspheres was investigated, after intra-myocardial injection.[18] Microspheres were identified in the lungs,[19] even when microspheres of large size that were expected to be completely retained in the heart were used, suggesting that pre-capillary arterio-venous shunts that bypass the low diameter capillaries probably underlie this phenomenon.[20] Egress via lymphatics may only play a small role 1 hour after injection because of low motility and filtering by lymph nodes between the heart and the lungs,[21–23] but could partially explain, progressive cell loss observed in the first 24 hours after transplantation.

In our study, we found large numbers of CDCs trapped in the lungs after intra-myocardial, intracoronary, and intravenous injections (Table 1) in contrast to a previous study using bone marrow-derived mononuclear cells, which found no cells in the lungs 1 hour post-intracoronary delivery.[24] This discrepancy can be attributed to differences in cell size between CDCs and mononuclear cells. Rat CDCs vary in size from 4 to 13 μm (Figure 4A; Supplemental Figure 4) following trypsinization, which would lead to trapping of larger cells that phenotypically resemble mesenchymal stem cells (MSCs),[7,25] in the microcirculation of the heart and the lungs (via pre-capillary AV shunts), following intravascular delivery (Figure 4B), since capillary diameter is ~4–5 μm in rats[26] (5–10 μm in

humans[27]). Widespread trapping of injected stem cells in the coronary and lung microvasculature could abrogate the functional benefits of stem cell therapy in the heart and lead to acute impairment of lung function, respectively. It is also possible that un-intentional stem cell delivery to the lungs may have a direct, salutary effect on lung function, as in the case of intravenous MSC transplantation.[28,29] Hence, detailed dose-response and coronary flow reserve measurements are needed in preclinical large animal studies and in clinical trials.

Furthermore, since CDCs are comprised a mixture of cell types, including a subset of cardiac MSCs[7,25] this explains our results of ~50%–60% combined cell retention in heart and lungs, in the PL, AI-RM, NL, and AI-RV groups, with the remainder of the smaller cells probably being widely distributed in the rest of the organs.

In animals receiving intra-myocardial CDCs, we believe that the presence of CDCs in the lungs cannot be attributed to technical factors. We took great care to avoid injecting cells into the right ventricle and only areas of the lateral left ventricular wall were selected for cell delivery. We found evidence for CDC transit through the cardiac venous system both visually and following the use of Di-I labeled rCDCs and Thioflavin S-labeled cardiac vasculature.

In animals receiving intra-myocardial injections, although accumulation of CDCs in the lungs was observed in the permanent ligation (Figure 2A), ischemia reperfusion (Figure 2B–D) and non-infarcted animals, a larger proportion of CDCs ended up in the lungs, in animals subjected to ischemia-reperfusion and in non-infarcted ones, suggesting that perfusion at the injection site greatly influences CDC retention. An intact microcirculation in the normal group and reactive hyperemia in the ischemia-reperfusion group are probably responsible for this phenomenon. Previous studies[30] have demonstrated that maximal hyperemia is observed immediately after restoration of blood flow and then declines progressively toward baseline flow levels, over a period of time that is determined by the duration of the ischemic insult. In our study, rCDCs were injected during this maximal hyperemia phase, when high blood volumes and velocities may have facilitated the wash out of the cells into the coronary venous circulation and eventually into the lungs. Significant numbers of CDCs (albeit at lower levels) were also observed in the lungs of animals subjected to permanent ligation of the LAD. This may be explained by delivery of some cells to the border zone of the infarct, where perfusion was maintained by branches of the coronaries more proximal to the occlusion site and active propulsion of CDCs into the cardiac venous system by cardiac contraction. Again, microsphere studies have also documented particle migration even in models of permanent coronary artery ligation, further validating our findings.[6,31]

Low cardiac cell retention in combination with low numbers of cells in the lungs was observed in the CI-R and AI-RC groups. In the case of CI-R, thinning of the infarcted area could have been responsible for inadvertent injection of cells into the left ventricular cavity, resulting in low cell numbers in both heart and lungs. In the AI-RC group, inability to directly deliver cells into the coronaries probably resulted in loss of large numbers of cells into the systemic circulation.

CONCLUSION

Acute cardiac retention of transplanted CDCs varies with the myocardial substrate and injection route. Large numbers of transplanted CDCs are trapped in the lungs following intra-myocardial, intravenous, and intracoronary injections. Intra-myocardially injected CDCs escape into the lungs via the coronary venous system, an effect that is more pronounced in perfused myocardium. We are now investigating PET-guided, tissue engineering-based methods to improve acute cardiac retention, long-term engraftment, and functional benefits of transplantation.

Limitations

The results obtained in this small animal model may not reflect retention in humans because of lack of coronary artery disease and differences in the anatomy of the coronary microcirculation in this animal model. The experimental simulation of intracoronary injection does not involve selective catheterization of coronary arteries and therefore cell loss into the systemic circulation is unavoidable. In addition, due to the small volumes of injectate, clumping of cells can occur, resulting in increased cell trapping in the microcirculation of the heart and lungs. Lastly, long-term engraftment, and functional effects of acute cardiac and lung retention were not assessed in this study. However, previous studies by our group have demonstrated improved left ventricular ejection function following intra-myocardial injection (in the acute, permanent ligation, rat and mouse models[7,10]), but not following intracoronary injection (in the chronic, ischemia-reperfusion pig model[25]) of CDCs, suggesting that injection route, cell retention and myocardial substrate play an important role in functional benefit following CDC transplantation. Prior studies also revealed low levels (<5%) of cardiac engraftment at 3 weeks,[8,25] and cell retention in lungs 4 days following intra-myocardial cell transplantation (data not shown).

Supplementary Material

Refer to Web version on PubMed Central for supplementary material.

Acknowledgments

This study was supported by the WW Smith Foundation (West Conshohocken, PA) (MRA), Donald W Reynolds Foundation (Las Vegas, NV), AHA (Dallas, TX) (MRA), Maryland TEDCO (Columbia, MD) (MRA), NIH RO1 HL092985 (Bethesda, MD) (MRA and FB).

We are grateful to Dana Kemmer for administrative assistance, Michelle Leppo, BS and Junaid M. Afzal, MBBS, MS for help with experiments.

References

1. Wu JC, Abraham MR, Kraitchman DL. Current perspectives on imaging cardiac stem cell therapy. J Nucl Med. 2010; 51:128S–36S. [PubMed: 20395348]
2. Amado LC, Saliaris AP, Schuleri KH, St John M, Xie JS, Cattaneo S, et al. Cardiac repair with intramyocardial injection of allogeneic mesenchymal stem cells after myocardial infarction. Proc Natl Acad Sci USA. 2005; 102:11474–9. [PubMed: 16061805]
3. Losordo DW, Schatz RA, White CJ, Udelson JE, Veereshwarayya V, Durgin M, et al. Intramyocardial transplantation of autologous CD34+ stem cells for intractable angina: A phase

I/IIa double-blind, randomized controlled trial. Circulation. 2007; 115:3165–72. [PubMed: 17562958]

4. Tse HF, Kwong YL, Chan JK, Lo G, Ho CL, Lau CP. Angiogenesis in ischaemic myocardium by intramyocardial autologous bone marrow mononuclear cell implantation. Lancet. 2003; 361:47–9. [PubMed: 12517468]
5. Hofmann M, Wollert KC, Meyer GP, Menke A, Arseniev L, Hertenstein B, et al. Monitoring of bone marrow cell homing into the infarcted human myocardium. Circulation. 2005; 111:2198–202. [PubMed: 15851598]
6. Suzuki K, Murtuza B, Beauchamp JR, Brand NJ, Barton PJ, Varela-Carver A, et al. Role of interleukin-1beta in acute inflammation and graft death after cell transplantation to the heart. Circulation. 2004; 110:II219–24. [PubMed: 15364866]
7. Smith RR, Barile L, Cho HC, Leppo MK, Hare JM, Messina E, et al. Regenerative potential of cardiosphere-derived cells expanded from percutaneous endomyocardial biopsy specimens. Circulation. 2007; 115:896–908. [PubMed: 17283259]
8. Terrovitis J, Lautamaki R, Bonios M, Fox J, Engles JM, Yu J, et al. Noninvasive quantification and optimization of acute cell retention by in vivo positron emission tomography after intra-myocardial cardiac-derived stem cell delivery. J Am Coll Cardiol. 2009; 54:1619–26. [PubMed: 19833262]
9. Kang WJ, Kang HJ, Kim HS, Chung JK, Lee MC, Lee DS. Tissue distribution of 18F-FDG-labeled peripheral hematopoietic stem cells after intracoronary administration in patients with myocardial infarction. J Nucl Med. 2006; 47:1295–301. [PubMed: 16883008]
10. Davis DR, Zhang Y, Smith RR, Cheng K, Terrovitis J, Malliaras K, et al. Validation of the cardiosphere method to culture cardiac progenitor cells from myocardial tissue. PloS one. 2009; 4:e7195. [PubMed: 19779618]
11. Terrovitis J, Stuber M, Youssef A, Preece S, Leppo M, Kizana E, et al. Magnetic resonance imaging overestimates ferumoxide-labeled stem cell survival after transplantation in the heart. Circulation. 2008; 117:1555–62. [PubMed: 18332264]
12. Dawn B, Stein AB, Urbanek K, Rota M, Whang B, Rastaldo R, et al. Cardiac stem cells delivered intravascularly traverse the vessel barrier, regenerate infarcted myocardium, and improve cardiac function. Proc Natl Acad Sci USA. 2005; 102:3766–71. [PubMed: 15734798]
13. Helmchen F, Denk W. Deep tissue two-photon microscopy. Nat Methods. 2005; 2:932–40. [PubMed: 16299478]
14. Honig MG, Hume RI. Fluorescent carbocyanine dyes allow living neurons of identified origin to be studied in long-term cultures. J Cell Biol. 1986; 103:171–87. [PubMed: 2424918]
15. Schlegel JU. Demonstration of blood vessels and lymphatics with a fluorescent dye in ultraviolet light. Anat Rec. 1949; 105:433–43. incl 2 pl. [PubMed: 15409572]
16. Hou D, Youssef EA, Brinton TJ, Zhang P, Rogers P, Price ET, et al. Radiolabeled cell distribution after intramyocardial, intracoronary, and interstitial retrograde coronary venous delivery: Implications for current clinical trials. Circulation. 2005; 112:I150–6. [PubMed: 16159808]
17. Anderl JN, Robey TE, Stayton PS, Murry CE. Retention and biodistribution of microspheres injected into ischemic myocardium. J Biomed Mater Res A. 2009; 88:704–10. [PubMed: 18335529]
18. Grossman PM, Han Z, Palasis M, Barry JJ, Lederman RJ. Incomplete retention after direct myocardial injection. Catheter Cardiovasc Interv. 2002; 55:392–7. [PubMed: 11870950]
19. Teng CJ, Luo J, Chiu RC, Shum-Tim D. Massive mechanical loss of microspheres with direct intramyocardial injection in the beating heart: Implications for cellular cardiomyoplasty. J Thorac Cardiovasc Surg. 2006; 132:628–32. [PubMed: 16935119]
20. Andersen KS, Skjerven R, Lekven J. Stability of 8-, 15-, and 26-micron microspheres entrapped in feline myocardium. Am J Physiol. 1983; 244:H121–30. [PubMed: 6849399]
21. Altman PA, Sievers R, Lee R. Exploring heart lymphatics in local drug delivery. Lymphat Res Biol. 2003; 1:47–53. discussion 4. [PubMed: 15624321]
22. Ludwig J. Trapping of calibrated microspheres in rat lymph nodes. Lymphology. 1971; 4:18–24. [PubMed: 5576118]
23. Castronuovo JJ Jr, Lopez-Majano V, Flanigan P, Schuler JJ, Jonasson O. Cardiovascular lymphoscintigraphy. Surgery. 1983; 94:351–7. [PubMed: 6879449]

24. Blocklet D, Toungouz M, Berkenboom G, Lambermont M, Unger P, Preumont N, et al. Myocardial homing of nonmobilized peripheral-blood CD34+ cells after intracoronary injection. Stem Cells. 2006; 24:333–6. [PubMed: 16223854]
25. Johnston PV, Sasano T, Mills K, Evers R, Lee ST, Smith RR, et al. Engraftment, differentiation, and functional benefits of autologous cardiosphere-derived cells in porcine ischemic cardiomyopathy. Circulation. 2009; 120:1075–83. 7. following 83. [PubMed: 19738142]
26. Henquell L, LaCelle PL, Honig CR. Capillary diameter in rat heart in situ: Relation to erythrocyte deformability, O2 transport, and transmural O2 gradients. Bibliotheca anatomica. 1977:416–9. [PubMed: 597184]
27. Brown, SP.; Miller, WC.; Eason, JM. Exercise physiology: Basis of human movement in health and disease. Baltimore: Lippincott Williams & Wilkins; 2006.
28. Hare JM, Traverse JH, Henry TD, Dib N, Strumpf RK, Schulman SP, et al. A randomized, double-blind, placebo-controlled, dose-escalation study of intravenous adult human mesenchymal stem cells (prochymal) after acute myocardial infarction. J Am Coll Cardiol. 2009; 54:2277–86. [PubMed: 19958962]
29. Lee RH, Pulin AA, Seo MJ, Kota DJ, Ylostalo J, Larson BL, et al. Intravenous hMSCs improve myocardial infarction in mice because cells embolized in lung are activated to secrete the anti-inflammatory protein TSG-6. Cell Stem Cell. 2009; 5:54–63. [PubMed: 19570514]
30. Coffman JD, Gregg DE. Reactive hyperemia characteristics of the myocardium. Am J Physiol. 1960; 199:1143–9. [PubMed: 13694286]
31. Feygin J, Mansoor A, Eckman P, Swingen C, Zhang J. Functional and bioenergetic modulations in the infarct border zone following autologous mesenchymal stem cell transplantation. Am J Physiol Heart Circ Physiol. 2007; 293:H1772–80. [PubMed: 17573463]

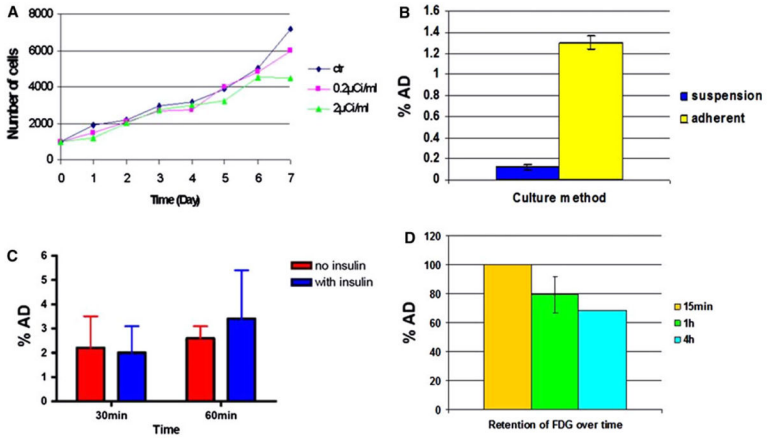

Figure 1.

Optimization of FDG uptake from rCDCs and effect of ^{18}FDG on CDC viability. **A** Effect of two ^{18}FDG doses (μCi of ^{18}FDG per mL of media) on CDC viability and proliferation rate. **B** ^{3}H[FDG] uptake by adherent and suspended rCDCs. **C** ^{3}H[FDG] uptake by rCDCs after 30- and 60-minute incubation with insulin. **D** ^{3}H[FDG] retention by rCDCs after 15-minute, 1-hour, and 4-hour incubation with ^{3}H[FDG].

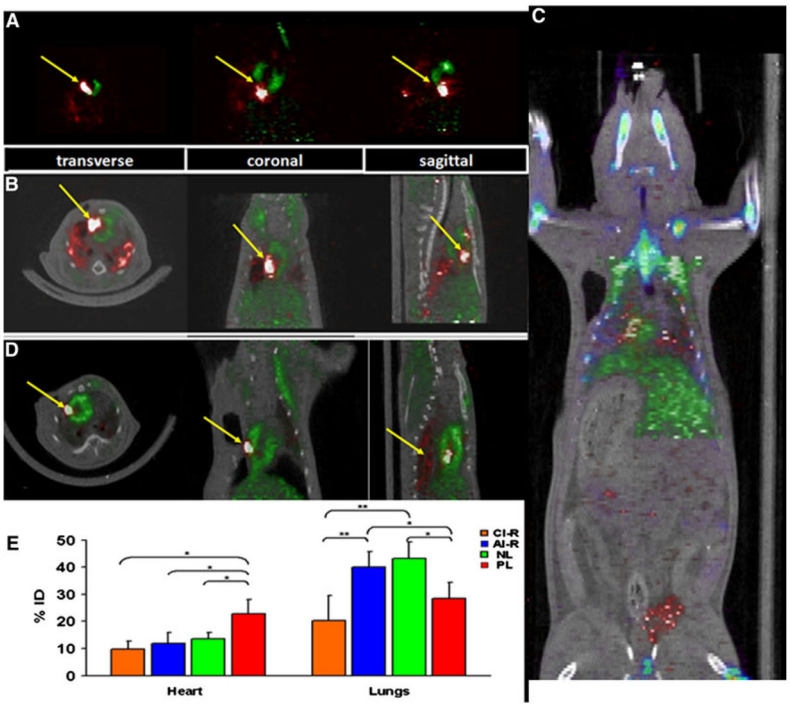

Figure 2.

In vivo PET/CT imaging ^{18}FDG-labeled rCDCs are identified as *bright spots* and indicated by *yellow arrows*. Myocardium (*green*), delineated by ^{13}NH3. **A** *PL group* permanent ligation of LAD with intra-myocardial rCDC injection; **B** *AI-RM group* acute-ischemia reperfusion followed by intra-myocardial rCDC injection. **C** *Whole body PET scan in AI-RM group* in addition to CDCs in the heart and the lungs, some FDG activity can be identified in the bladder (probably representing free ^{18}FDG released by dead cells). The liver (*green*) takes up substantial amounts of ^{13}NH3. **D** *CI-R group* chronic infarction induced by ischemia-reperfusion of LAD with intra-myocardial rCDC injection. **E** Heart and lung retention, measured by PET, 1 hour after intra-myocardial rCDC injection in the PL, AI-RM, NL, and CI-R groups. *ID*, injected dose (*$P < .05$).

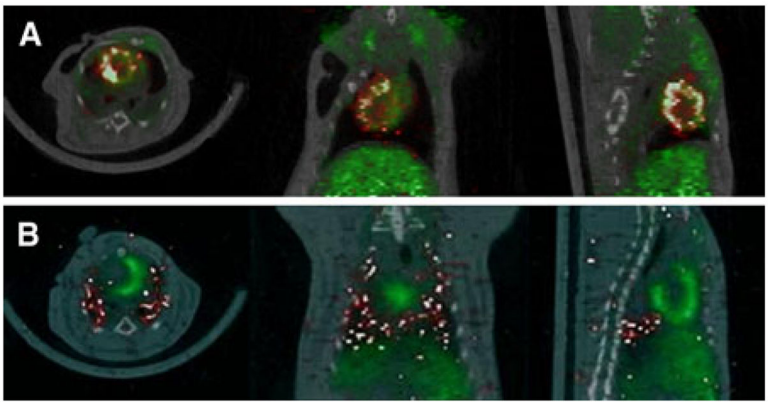

Figure 3.

Quantitative in vivo PET results. **A** In vivo PET/CT imaging following intracoronary rCDC injection. *Yellow arrows* indicate ^{18}FDG-labeled rCDCs; myocardium (*green*) is delineated by $^{13}NH_3$. **B** In vivo PET/CT imaging following intravenous rCDC injection. *Yellow arrows* indicate ^{18}FDG-labeled CDCs; myocardium (*green*) is delineated by $^{13}NH_3$.

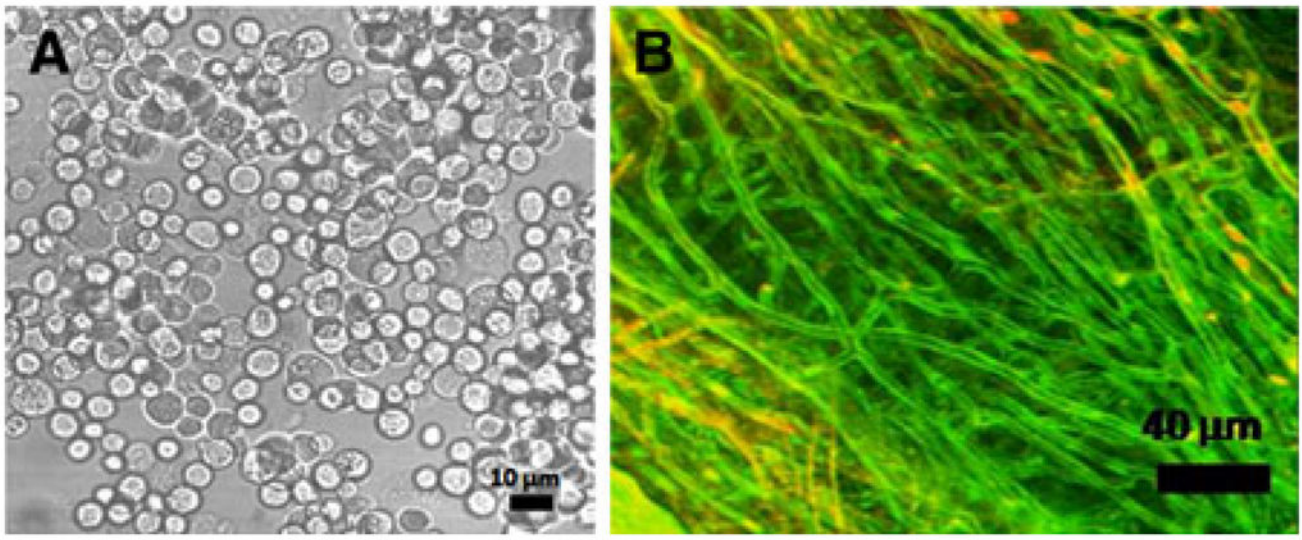

Figure 4.

Two photon microscopy **A** Transmitted light images of rCDCs following trypsinization. **B** Two-photon imaging of rat myocardial capillaries stained with Thioflavin-S.

Table 1

Description of study groups

Transplantation route	Transplanted cell number	Cardiac retention	Lung retention
Intra-myocardial injection			
Permanent ligation (PL), n = 15 Cell transplantation immediately following ligation	2×10^6	22.9% ± 5.2%	28.5% ± 5.0%
Acute ischemia-reperfusion (AI-RM), n = 17 Ischemia for 45 minutes followed by reperfusion and immediate cell transplantation	2×10^6	12.0% ± 3.9%	39.9% ± 9.3%
Normal (NL), n = 10 Cell transplantation without infarction	2×10^6	13.6% ± 2.3%	43.3% ± 5.6%
Chronic ischemia-reperfusion (CI-R), n = 13 Ischemia for 45 minutes followed by reperfusion; cell transplantation 30 days after reperfusion	2×10^6	9.9 ± 2.8	20.2% ± 9.3%
Intracoronary (intra-cavitary) injection			
Acute ischemia-reperfusion (AI-RC), n = 5 Ischemia for 45 minutes followed by reperfusion and immediate cell transplantation	1×10^6	15.4% ± 5.5%	19.9% ± 5.6%
Intravenous injection			
Acute ischemia-reperfusion (AI-RV), n = 10 Ischemia for 45 minutes followed by reperfusion and immediate cell transplantation	5×10^6	0.8% ± 1.06%	55.1% ± 9.3%